Probability Density Function modelling of molecular mixing in flames with differential diffusion

E.S. Richardson[1,*], J.H. Chen[2]

[1] University of Southampton, Faculty of Engineering and the Environment, University Road, Southampton, SO17 1BJ, UK, e.s.richardson@soton.ac.uk

[2] Sandia National Laboratories, Combustion Research Facility, PO Box 969, Livermore, California, 94551-0969, USA, jhchen@sandia.gov

Abstract

Motivated by the fact that differential diffusion can affect pollutant emission and flame stability in practical combustion systems, this paper presents a modified Euclidean Minimum Spanning Tree mixing model which accounts for differential diffusion. The new Probability Density Function modelling satisfies requirements of realizability and conservation of mass, and validation is conducted by comparison with Direct Numerical Simulation data.

Introduction

Modelling of turbulent reacting flows requires closure for averaged or filtered chemical source terms. Probability density function (PDF) methods (1) provide an exact closure for chemical reaction rates but molecular mixing terms remain unclosed and must be modelled. Under particular conditions, for example in the presence of flames, modelling for the effects of molecular mixing on the composition PDF can be deficient (2). Attempts have been made to address aspects of mixing associated with flames, such as localness (3; 4) and differential diffusion (5; 6).

In the flamelet regime of turbulent premixed combustion the scalar length scales are imposed predominantly by the reaction-diffusion balance in the flame front, rather than by the turbulence cascade process. It is observed from several DNS studies of mixing in homogeneous turbulence (7; 8) that, when the scalar length scales are controlled by the turbulence cascade process, the scalar dissipation rate is independent of species diffusivities, and proportional to the turbulent frequency, $\omega = \epsilon/k$ (where ϵ is the dissipation rate of turbulent kinetic energy k). The simulations by Juneja and Pope (7) are initialized with a scalar field which is independent from the turbulent field. In this situation, they observe that the *initial* scalar dissipation rates depend on the length scales characterising the scalar fields (shorter length scales increase the scalar dissipation rate), and on the species diffusivities (higher diffusivities increase the scalar dissipation rate). Because, in flamelet combustion, the scalar length scales are not controlled only by the turbulence cascade process, we expect the scalar dissipation rate to depend partly on the flame length scales, and, consequently, on the molecular diffusivities of the individual scalars as well. This causes scalar dissipation rates to differ among species (9; 10). The transition between flamelet premixed combustion and distributed premixed combustion is delineated indicatively by a Karlovitz number (Ka) of order unity (11). Because the Karlovitz number can be varied independently from the Reynolds number, it is important to note that flamelet combustion, and effects of the associated differential diffusion processes, can occur even at high Reynolds number, provided that Ka is small.

Specific Objectives

The specific objectives of this paper are two-fold: (i) to present a new variant of the Euclidean Minimum Spanning Tree (EMST) mixing model (3) which accounts for differential diffusion while satisfying appropriate realizability constraints; and (ii) to use Direct Numerical Simulation (DNS) data for a turbulent premixed Bunsen flame to compare the performance of the new EMST model with the standard EMST and Interaction by Exchange with the Mean (IEM) (12) models.

The EMST-DD model for differential diffusion

Meyer (6) provides a summary of the performance of a comprehensive selection of mixing models. From Meyer's comparison, the EMST model is the only multi-scalar mixing model which enforces scalar-localness. Because the localness property is important in flamelet combustion (where differential diffusion is also expected to be important) we choose to develop the EMST model to account for differential diffusion. PDF mixing models that have been applied to differential diffusion previously (6; 13) are problematic because these mixing models guarantee neither conservation of means nor that the sum of mass fractions remains equal to unity (the latter is a *realizability* constraint).

A complete description of the EMST mixing model is provided by Subramaniam and Pope (3). The EMST model describes the mixing among an ensemble of notional particles that are used to represent the composition-PDF. Pairwise mixing occurs along branches of a Minimum Spanning Tree, constructed in composition space. The contribution to the change of the mass fraction $\mathrm{Y}_\alpha^{(\mathrm{p})}$ of species α on the notional particle (p), due solely to the mixing along the branch connecting particles (p) and (q),

*Corresponding author: e.s.richardson@soton.ac.uk

is given by:

$$\mathrm{w}^{(\mathrm{p})}\frac{\mathrm{dY}_{\alpha}^{(\mathrm{p})}}{\mathrm{dt}} = -\mathrm{aB}_{\mathrm{pq}}(\mathrm{Y}^{(\mathrm{p})} - \mathrm{Y}^{(\mathrm{q})}). \qquad (1)$$

The overall rate of change of $\mathrm{Y}_{\alpha}^{(\mathrm{p})}$ is given by summing the contributions, evaluated using Eq. 1, from every particle (q) connected to directly to particle (p) by the Minimum Spanning Tree. $\mathrm{w}^{(\mathrm{p})}$ is the statistical weight of particle (p), 'a' is a global mixing coefficient, and B_{pq} is a mixing coefficient that depends on the location of the branch (pq) within the tree. In the standard EMST mixing model, the mixing coefficients are the same for every species. The EMST-Differential Diffusion (EMST-DD) model accounts for differential diffusion by introducing an additional mixing coefficient, C_{α}, whose value can be different for each species, in a manner which depends on the diffusivities of the individual species. To ensure that the EMST-DD model enforces realizability, a correction term is required so that all M mass fractions evolve according to:

$$\begin{aligned}\mathrm{w}^{(\mathrm{p})}\frac{\mathrm{dY}_{\alpha}^{(\mathrm{p})}}{\mathrm{dt}} &= -\mathrm{aC}_{\alpha}\mathrm{B}_{\mathrm{pq}}(\mathrm{Y}_{\alpha}^{(\mathrm{p})} - \mathrm{Y}_{\alpha}^{(\mathrm{q})}) \qquad (2)\\ &+ \mathrm{Y}_{\alpha}^{(\mathrm{p})}\sum_{\beta=1}^{\mathrm{M}}\mathrm{aC}_{\beta}\mathrm{B}_{\mathrm{pq}}(\mathrm{Y}_{\beta}^{(\mathrm{p})} - \mathrm{Y}_{\beta}^{(\mathrm{q})}).\end{aligned}$$

The correction term in Eq. 2 is analogous to the correction velocity that is employed in some models for the diffusion velocities in systems with differential diffusion (page 16, in ref. (14)). Summing Eq. 2 over all species gives $\mathrm{d}\{\sum_{\alpha}\mathrm{Y}_{\alpha}^{(\mathrm{p})}\}/\mathrm{dt} = 0$, as required for realizability. The individual mass fractions also remain bounded by zero since the second term on the right hand side in Eq. 2 tends to zero as $\mathrm{Y}_{\alpha}^{(\mathrm{p})}$ approaches zero, and the first term on the right hand side is known to satisfy realizability constraints provided that the mixing coefficients are all positive (3). Since Eq. 2 ensures that the mass fractions are non-negative and that they sum to unity, the correction term also ensures that the individual species mass fractions can not exceed unity.

Conservation of means then requires an exchange of particle weight given by,

$$\frac{\mathrm{dw}_{\alpha}^{(\mathrm{p})}}{\mathrm{dt}} = -\sum_{\beta=1}^{\mathrm{M}} a\mathrm{C}_{\beta}\mathrm{B}_{\mathrm{pq}}(\mathrm{Y}_{\beta}^{(\mathrm{p})} - \mathrm{Y}_{\beta}^{(\mathrm{q})}). \qquad (3)$$

According to Eq. 3 it is possible (although unlikely in practice) for some particle weights to decrease to zero. If the statistical weight of a particle decreases to zero it should be removed it from the ensemble.

The EMST-DD model does not guarantee that all species variances decay since the second term on the right hand side of Eq. 2 may have a magnitude greater than the first. The possibility of predicting scalar variance production by molecular mixing – which at first sight may appear alarming – is physically permissible in the case of differentially diffusing mixtures. This claim can be verified by considering a premixed flame in which an inert species has the same mass fraction in the products and the reactants. The mass fraction of the inert species, however, can fluctuate within the flame front due to differential diffusion of other reactive species, thereby differential diffusion generates a variation of an initially uniform species mass fraction (this has been confirmed by computations of laminar premixed flames using multi-component transport models in ref. (15)).

If the joint-PDF of composition includes the specific enthalpy of the mixture, h, a correction term is required in order to achieve conservation of the mean specific enthalpy:

$$\begin{aligned}\mathrm{w}^{(\mathrm{p})}\frac{\mathrm{dh}^{(\mathrm{p})}}{\mathrm{dt}} &= -\mathrm{aC}_{\mathrm{h}}\mathrm{B}_{\mathrm{pq}}(\mathrm{h}^{(\mathrm{p})} - \mathrm{h}^{(\mathrm{q})}) \qquad (4)\\ &+ \mathrm{h}^{(\mathrm{p})}\sum_{\beta=1}^{\mathrm{M}}\mathrm{aC}_{\beta}\mathrm{B}_{\mathrm{pq}}(\mathrm{Y}_{\beta}^{(\mathrm{p})} - \mathrm{Y}_{\beta}^{(\mathrm{q})}).\end{aligned}$$

The changing particle weights also lead to a correction for the particle velocities. It is shown in Ref. (15) that conservation of mass, momentum and kinetic energy dictate that the particle velocities $\mathbf{u}^{(i)}$ evolve according to:

$$\frac{\mathrm{d}\mathbf{u}^{(\mathrm{p})}}{\mathrm{dt}} = \frac{\mathrm{dw}^{(\mathrm{p})}}{\mathrm{dt}}\left(\frac{\mathbf{u}^{(\mathrm{q})} - \mathbf{u}^{(\mathrm{p})}}{2\mathrm{w}^{(\mathrm{p})}}\right). \qquad (5)$$

A model for the functional form of the species-dependent mixing coefficients must now be specified. We propose the following model:

$$\mathrm{C}_{\alpha} = 1 + \mathrm{C}_{\mathrm{K}}(\frac{1}{\mathrm{Le}_{\alpha}} - 1), \qquad (6)$$

in which the species dependent mixing coefficients depend on the species Lewis numbers Le_{α}, and a model parameter C_{K} which takes a value between zero and unity. When C_{K} equals zero the standard EMST model is recovered. When C_{K} equals unity, the rate at which mass is transferred between two particles is proportional to the diffusivity and the scalar-difference between the pair, and 'differential mixing' occurs. Based on the discussion in the introduction, we expect differential diffusion to become important in the flamelet regime of combustion, and to be unimportant in high-Reynolds number mixing of inert or low-Damköhler number mixtures. This suggests that C_{K} should be a function of the combustion regime, for example, measured by the Karlovitz number: i.e. $\mathrm{C}_{\mathrm{K}} \rightarrow 0$ for Ka$\gg 1$, and $C_K \rightarrow 1$ for Ka$\ll 1$. In this investigation we do not specify a functional form for C_{K} but test a range of values.

Simulation configuration and methods

Turbulent flame DNS: A three-dimensional turbulent perfectly-premixed Bunsen flame has been analyzed in this study. The flame simulated by Sankaran *et al.* (16) comprises a planar jet of unburned methane and air at 800K, 1 atm and equivalence ratio ϕ=0.7 issuing into a coflowing product stream from adiabatic combustion of

the mixture. The DNS configuration is shown in Fig. 1. The slot jet width, H=1.8mm, the jet velocity (100ms^{-1}) and coflow velocity (25ms^{-1}) give a jet Reynolds number of 2100. The simulations were performed using the DNS code S3D, using a reduced chemical reaction model with 13 species (17), and constant, non-unity Lewis number transport (except for N_2 which makes up the balance of the composition). Full details of the simulation are presented by Richardson *et al.* (9).

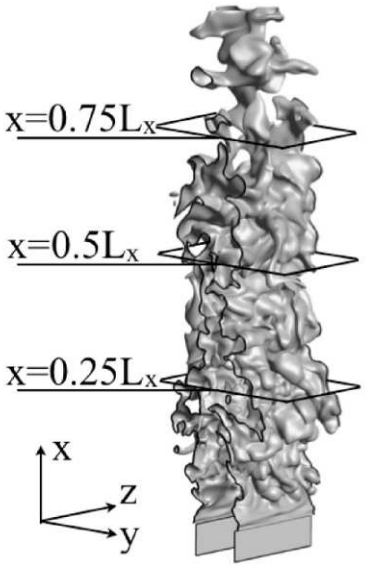

Figure 1: Premixed flame DNS configuration, showing an instantaneous iso-surface for progress variable = 0.65.

PDF simulation method: The premixed Bunsen configuration has also been simulated using a one-dimensional transported PDF approach, implemented using Lagrangian particles. The PDF calculations use the mean velocity field, the turbulent kinetic energy, and the Favre averaged dissipation rate taken from the DNS. The PDF computations exploit the statistical homogeneity along the z-direction, and symmetry around the y=0 plane in the DNS configuration. Further simplification is made by employing a one-dimensional PDF domain (which extends across half of the y-direction in the DNS domain), and integrating the PDF equations in spatial increments along the x-direction (by assuming that the time increments $\Delta t = \Delta x/\tilde{U}$, where $\tilde{U}$ is the mean axial velocity from the DNS). The cross-stream positions of the particles are advanced using the simplified Langevin model for particle acceleration (18). This simple parabolic solution method cannot be expected to give accurate predictions of the mean flame shape in general. Here we report conditional statistics, and ratios of mixing timescales, which are relatively insensitive to the overall flame shape, and which permit a useful comparison between micro-mixing models. PDF simulation data are presented for the IEM, EMST, and EMST-DD models. The PDF simulation is initialized at 3.3 jet heights from the nozzle, and the results are reported at 6.6H (cf. x/L_x in Fig. 1.

Results and Discussion

Analysis of the DNS simulation (9) indicates that combustion occurs in the thickened flame regime (11). The analysis by Richardson *et al.* (9) shows that the non-unity ratios between species mixing rates, shown in Fig. 2a, are due to the presence of premixed flames. In this study, the scalar dissipation rate is evaluated as $\chi_\alpha = -2\widetilde{Y''_\alpha \Gamma_\alpha}$ [from Eq. B.2 in Ref. (19)], where Γ_α is the diffusion source term. An occurrence of $\chi_\alpha < 0$ indicates variance production due to differential diffusion (as discussed in the section on the EMST-DD model). Note that further simplification to the commonly used expression for scalar dissipation $\chi_\alpha = 2D_\alpha \widetilde{(\nabla Y''_\alpha)^2}$, where D_α is the species' diffusivity, requires assumptions of Fickian diffusion with equal diffusivities, and we do not make these assumptions in this study. We define the species mixing rate as $\Lambda_\alpha = \tilde{\chi_\alpha}/\tilde{Y''^2_\alpha}$. Ratios of $\Lambda_\alpha/\Lambda_{O_2}$ for $\alpha \in \{H_2, H, OH, CO, N_2\}$ are also shown for the EMST and EMST-DD models in Fig. 2. Note that the IEM model gives identical Λ_α for all species, and it is not plotted. The EMST model predicts mixing ratios which are close to unity at the centre of the flame brush (y/H≈0.5 at the axial location of x=6.6H which is plotted). The EMST-DD model gives greatly improved prediction of the relative species mixing rates. The EMST-DD data are shown for $C_K = 0.3$ which gives close agreement with the DNS mixing rates.

Diffusion rates of Y_{CO}, sampled from across the y-direction at x=6.6H, are plotted in Fig. 3 for DNS, IEM, and EMST simulations. Data are plotted versus the progress variable sample space variable ζ, where progress variable (equal to zero in reactants and unity in the products) has been based on Y_{O2}. The IEM model fails to predict the structure of the diffusion process in progress variable-space. The EMST model gives a distribution of mixing rates which have the same shape as the DNS. The frequent occurrence of zero mixing in the EMST is due to the model's intermittency feature described in (3). The species dependent mixing coefficients in Eq. 2 then serve to adjust the relative magnitude of the species mixing terms, resulting in the improved predictions of the mixing rate ratios seen in Fig. 2.

Differential diffusion is responsible for the curvature of the conditional mean Y_{H_2} profile, in the non-reactive mixture of the pre-heat zone (ζ <0.5), which is seen for the DNS data in Fig. 4a. Since there is no chemical reaction in this mixture, the curvature arises because Y_{H_2} diffuses faster into the reactants than the diffusion of progress variable itself. Over the same range of ζ, the EMST model predicts a linear variation of the conditional mean. The EMST-DD, however, produces accurate predictions of the conditional mean and rms of Y_{H_2} for $\zeta < 0.5$. The conditionally averaged Y_{H_2} diffusion rates in Fig. 4b also shows that the EMST-DD model improves upon the predictions of the standard EMST. EMST pre-

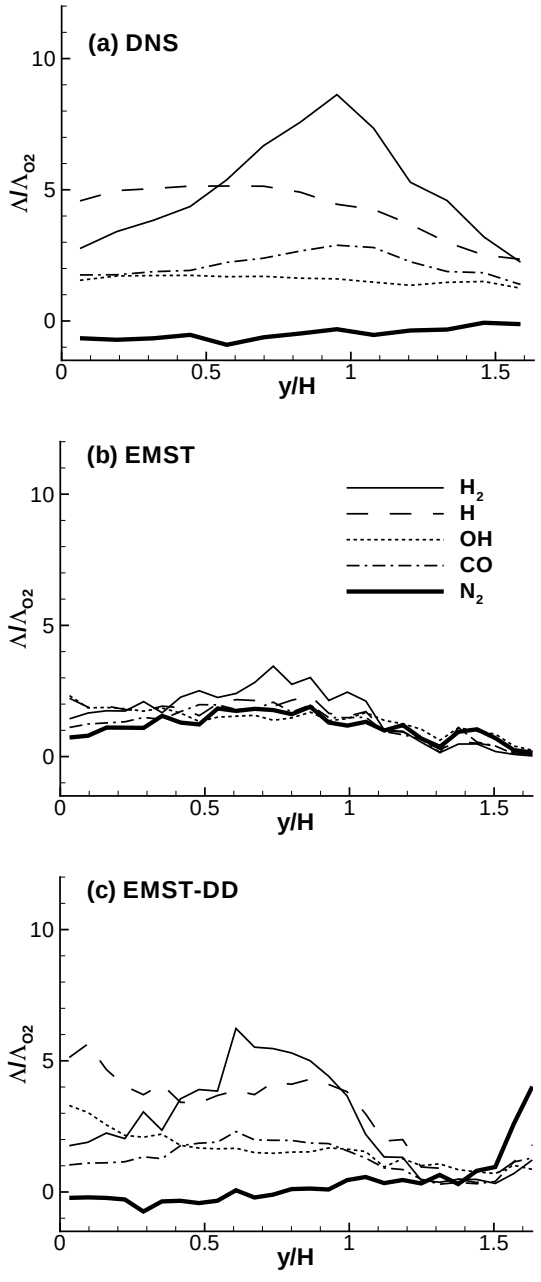

Figure 2: Ratios for Λ between selected species (H_2, H, OH, CO, N_2) and O_2 in the (a) DNS, (b) EMST, and (c) EMST-DD simulations.

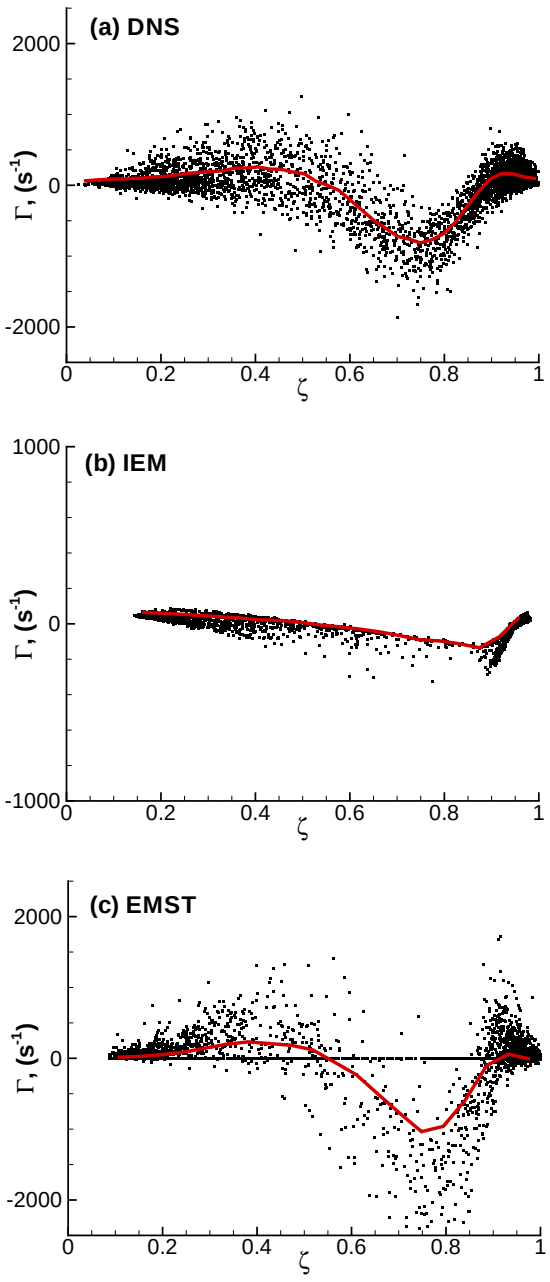

Figure 3: Diffusion rates of CO in progress variable space from (a) the DNS, (b) IEM, and (c) EMST simulations. The solid line is the conditional mean.

dictions of the conditional average CO and O_2 mass fraction and diffusion rates in Fig. 4 are changed little by the differential diffusion correction, and they agree with the DNS data closely.

Variation of the Y_{N_2} conditional mean mass fraction is shown in Fig. 4e. There is a finite variation in of Y_{N_2} in the initial condition of the PDF calculations, and this persists even in the case of the EMST model. The effect of differential diffusion is seen in the DNS and EMST-DD profiles, where differential diffusion moves Y_{N_2} from the preheat-zone into the reactant zone, generating variance. While the variation of Y_{N_2} is small, and unlikely to have any practical significance in a combustion system, we note that the EMST-DD model reproduces this feature which is symptomatic of differential diffusion. We note also that the EMST-DD reproduces the negative values, and the shape of the cross-stream variation, of the $\Lambda_{N_2}/\Lambda_{O_2}$ mixing ratio seen in the DNS in Fig. 2.

Conclusions

An extension of the EMST mixing model has been presented which accounts for differential diffusion. To the authors' knowledge this is the first PDF mixing model which accounts for differential diffusion in a manner which conserves mass and enforces basic realizability constraints. The new EMST-DD model retains most other advantages (e.g. *localness*), and limitations, of the standard EMST model. A remarkable novel feature of the EMST-DD model is that it permits differential diffusion to produce scalar variance.

The performance of the EMST-DD, EMST, and IEM models has been assessed by comparison of conditional statistics and mixing timescales with DNS data for a premixed turbulent Bunsen flame. Unlike the IEM model, the EMST models describe the structure of mixing through the flame correctly. Combining the EMST description of scalar localness with differential mixing rates, the EMST-DD model, predicts mixing rate ratios similar to those in the DNS. The EMST-DD correctly predicts that variance of Y_{N_2} is produced in the premixed combustion DNS.

This study has demonstrated that the EMST-DD model predictions exhibit successfully several features which characterize flamelet combustion with differential diffusion. The modelling for the parameter C_K remains to be determined in general, and the modelling now requires further validation across a broader range of mixing regimes.

Acknowledgements

This work was supported by the Division of Chemical Sciences, Geosciences and Bio-sciences, the Office of Basic Energy Sciences, the U.S. Department of Energy. Sandia National Laboratories is a multiprogram laboratory operated by Sandia Corporation, a Lockheed Martin Company, for the U.S. Department of Energy [contract number DE-AC04-94-AL85000]; and E.S. Richardson received further support from the UK Engineering and Physical Sciences Research Council [grant number EP/I004564/1]. In addition, the authors would like to thank Stephen B. Pope for helpful comments, and Fabrizio Bisetti for providing part of the PDF simulation program.

References

[1] S.B. Pope, Prog. Energy Combust. Sci. 11 (1985) 119-192.

[2] A.T. Norris, S.B. Pope, Combust. Flame 83 (1991) 27-42.

[3] S. Subramaniam, S.B. Pope, Combust. Flame 115 (1998) 487-514.

[4] M.J. Cleary, A.Y. Klimenko, J. Janicka, M. Pfitzner, Proc. Combust. Inst. 32 (2009) 1499-1507.

[5] J.-Y. Chen, W.-C. Chang, Combust. Sci. Technol. 133 (4) (1998) 343-375.

[6] D.W. Meyer, Phys. Fluids, 22 (2010) 035103.

[7] A. Juneja, S.B. Pope, Phys. Fluids 8 (1996) 2161-2184.

[8] P.K. Yeung, S.B. Pope, Phys. Fluids A. 5 (1993) 2467-2478.

[9] E.S. Richardson, R. Sankaran, R.W. Grout, J.H. Chen, Combust. Flame 157 (3) (2010) 506-515.

[10] E.R. Hawkes, R. Sankaran, J.C. Sutherland, J.H. Chen, Proc. Combust. Inst. 31 (2007) 16331640.

[11] N. Peters, Turbulent Combustion, Cambridge University Press, Cambridge, 2000, p.79.

[12] C. Dopazo, Phys. Fluids A 18 (4) (1975) 397-404.

[13] H. Chen, S. Chen, R.H. Kraichnan, Phys. Rev. Lett. 63 (Dec 1989) 2657-2660.

[14] T.Poinsot, D. Veynante, Theoretical and Numerical Combustion, Second Edition (R.T. Edwards Inc., Philadelphia, 2005).

[15] E.S. Richardson, J.H. Chen, Submitted to Combustion and Flame (2011).

[16] R. Sankaran, E.R. Hawkes, C.S. Yoo, J.H. Chen, T. Lu, C.K. Law, in: 5th U.S. National Combustion Meeting, 2007 B09.

[17] R. Sankaran, E.R. Hawkes, J.H. Chen, T. Lu, C.K. Law, Proc. Combust. Inst. 31 (1) (2007) 1291-1298.

[18] S.B. Pope, Turbulent Flows, Cambridge University Press, Cambridge, 2000, p.547.

[19] D.C. Haworth, Prog. Energy Combust. Sci. 36 (2) (2010) 168-259.

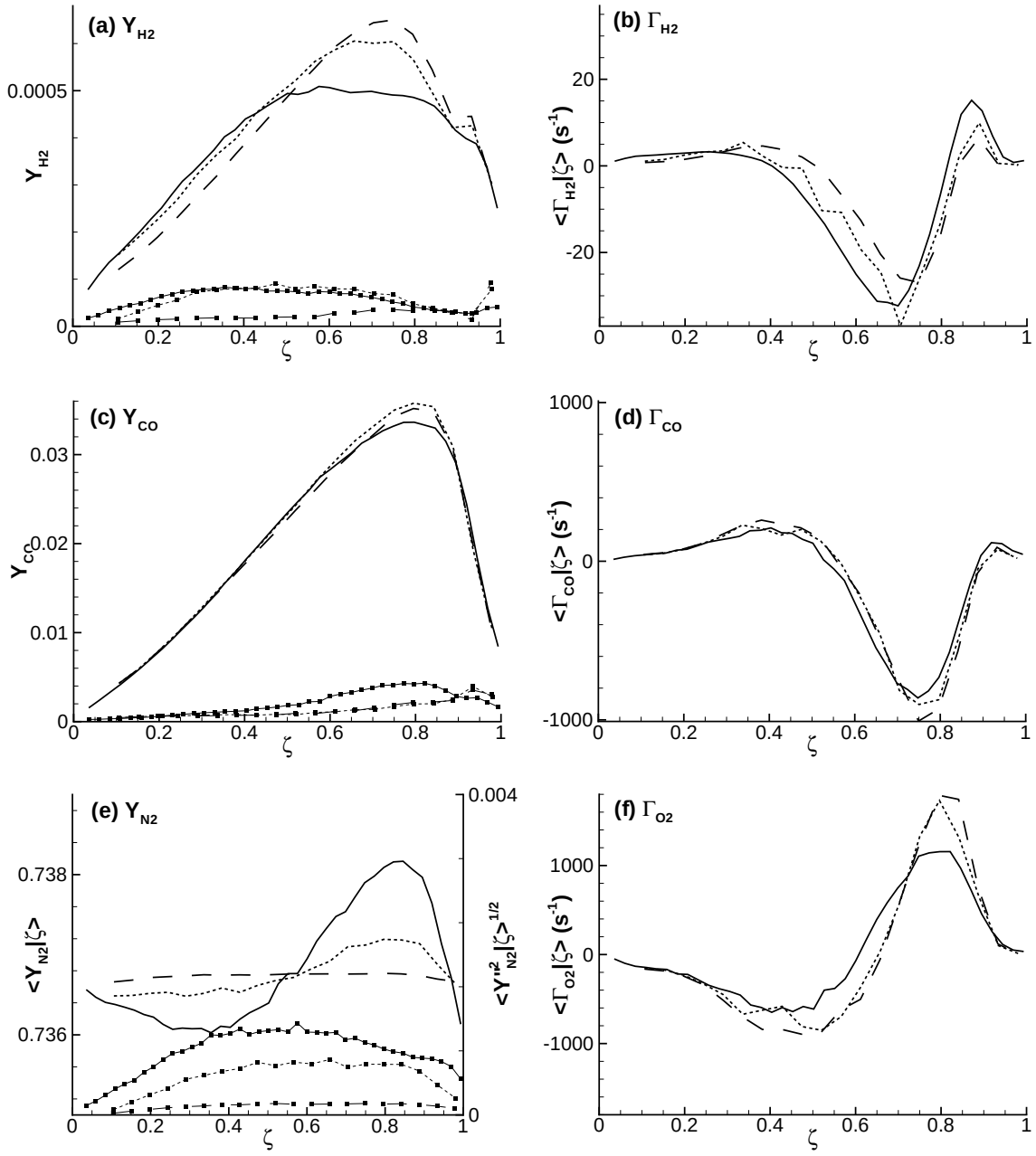

Figure 4: DNS (solid lines), EMST (dashes), and EMST-DD (dots) data for conditional mean (lines) and rms (lines with symbols) species mass fractions of H_2, CO, and N_2 (left column), and diffusion rates of H_2, CO, and O_2 (right column).